# EFFECT OF CANAL CURVATURE LOCATION ON THE CYCLIC FATIGUE RESISTANCE OF THE ENDOSEQUENCE CONTROLLED MEMORY FILE

by

Sarah Alghamdi

B.D.S, King Abdul-Aziz university, 2011

A THESIS SUBMITTED IN PARTIAL FULFILLMENT OF

THE REQUIREMENTS FOR THE DEGREE OF

MASTER OF SCIENCE

in

THE FACULTY OF GRADUATE AND POSTDOCTORAL STUDIES

(Craniofacial Science)

THE UNIVERSITY OF BRITISH COLUMBIA

(Vancouver)

August 2020

The following individuals certify that they have read, and recommend to the Faculty of Graduate and Postdoctoral Studies for acceptance, a thesis entitled:

**Effect of canal curvature location on the cyclic fatigue resistance of the new EndoSequence controlled memory file**

submitted by Sarah Alghamdi in partial fulfillment of the requirements for

the degree of Master of Science

in Craniofacial Science

**Examining Committee:**

Ya Shen, Associate professor, Department of Endodontics, UBC.
Supervisor committee

Dr. Markus Haapasalo, Professor, Chair, Department of Endodontics, UBC.
Supervisory Committee Member

Dr. Ahmed Hieawy, Clinical associate professor, Department of Endodontics, UBC.
Supervisory Committee Member

Dr. David McDonald, Professor, Chair, Oral and Maxillofacial Radiology.
Additional Examiner

## Abstract

**Introduction:** The study aim was to evaluate the effect of five different root canal curvature locations on the fatigue resistance of thermomechanically treated nickel-titanium (NiTi) files and traditional NiTi files at body temperature.

**Material and Methods:** EndoSequence (ES), EndoSequence (ESCM), K3, K3XF, and Vortex Blue (VB) NiTi files (size 25/.04) were subjected to fatigue testing inside artificial canals with a curvature of 60°, a 3-mm radius, and five different curvatures. Each instrument was rotated until fracture occurred. The number of cycles to failure ($N_f$) was recorded, the length of the fractured tips was measured, and the fractured surface of the fragments were examined by scanning electron microscopy. The phase transformation behaviour of NiTi files was also examined.

**Results:** ESCM files had the highest fatigue resistance, followed by the VB, K3XF, K3 and ES files ($p < 0.05$). Among the five curvature locations, ESCM files showed the highest $N_f$ of all the groups ($p < 0.05$), while either the ES or K3 files had the lowest $N_f$ ($p < 0.05$). Two endothermic peaks were observed on the heating curve of the heat-treated files (ESCM, K3XF, and VB).

**Conclusion**: The location of the canal curvature had a significant effect on both heat-treated and superelastic NiTi files. Instrumentation of canals with coronal curvature should be cautiously performed.

## Lay Summary

The main goal of endodontic treatment is the removal of the bacteria from the root canal system and elimination of infection. cleaning and debridement of the root canal with mechanical instrumentation and irrigation plays a major role in achieving this goal. Introduction of rotary NiTi files was considered a huge milestone in the history of Endodontics because they facilitated the shaping of curved root canals. Although NiTi rotary files are popular because of their flexibility and efficiency in root canal preparation, instrument fracture is a common occurrence that might have a negative impact on treatment outcome and patient satisfaction. Thus, the objective of this study was to study the cyclic fatigue resistance of EndoSequence controlled memory files, which are rotary files fabricated from a novel alloy shown to have improved flexibility in different curvature locations.

## Preface

This study was approved by the university of British Columbia Clinical Research Board (H12-02430) .This thesis is the principle work of the candidate, Sarah Alghamdi, as per the requirements of a Master of Science in Craniofacial Science with a Diploma in Endodontics. Sarah Alghamdi was responsible for performing the fatigue tests, preparing the file fragments for SEM, performing the DSC tests, interpretation and statistical analysis of the results, and writing of the thesis. The supervisor of this project, Dr. Ya Shen, contributed to the design of the study, analysis of the results, and editing of the thesis. Support and consultation were provided by Dr. Ahmed Hieawy and Dr. Markus Haapasalo. Jinghao Hu contributed to this project by obtaining the SEM images and providing support for statistical analysis. The relative contribution to this research project by Sarah Alghamdi was 80%.

## Table of Contents

## List of Tables

## List of Figures

## List of Abbreviations:

ADA: American Dental Association

$A_f$: Austenite transformation finish temperature

ANSI: American National Standards Institute

As: Austenite transformation start temperature

DSC: Differential scanning calorimetry

ES: EndoSequence

ESCM: EndoSequence controlled memory

ISO: International Organization for Standardization

$M_f$: Martensite transformation finish temperature

Ms: Martensite transformation start temperature

$N_f$: Number of cycles to failure

NiTi: Nickel titanium

rpm: Rotations per minute

$R_S$: R-phase transformation start temperature

SD: Standard deviation

SEM: Scanning electron microscope

VB: Vortex Blue

## Acknowledgements

I would like to thank my supervisor, Dr. Ya Shen, for her great support and encouragement. It was a great pleasure working with a leading researcher who also has a heart of gold, her warm smile and positivity were my motivation. I would like to also thank Drs. Markus Haapasalo and Ahmed Hieawy for their help and assistance, not only during my research but thought out my years of residency.

I would like to express my sincerest gratitude to Dr. Jeffery Coil who showed me how a true mentor and a human being should be. No words can describe my gratitude towards him and the opportunity he provided me with this program.

Thanks to Dr. Xiangya Huang, who made the fatigue test model for the project.

Also, I would like to thank Jinghao Hu for his help and support in the lab, as well as performing my results statistics. I would like to also thank Christophe Mobuchon and Sherry Kiafar who welcomed us into their lab and guided us during our DSC analysis. In addition, I would like to thank Angela Tether for her help and assistance in the scientific editing of my thesis.

Finally, I would like to thank my clinical instructors, the CDA staff, and my co-residents.

## Dedication

I dedicate this work to the most loving and devoted parents, my mom Zoubaida Naber and dad Saleh Alghamdi. Your unconditional love, sacrifice, devotion, and support is what made me who I am today. I am forever in your debt. Mom and dad, no words can describe my love and gratitude for you. All I wish is that I can be there for you as much as you were there for me and my children, and no matter what I do I can never repay you for what you did for me.

To my husband Hicham Elmouchaouq, who's strength and positivity gave me the strength to go through my years of residency and life.

To my little angels, my blessings, the loveliest gifts from god, Sulaiman, Laila, and Lana, everything I did was for you. I hope one day I will make you proud.

To my brothers, my rock and backbone, Ammr and Hatim.

# Chapter 1

## 1.1 Introduction

The foundation of endodontic treatment is the successful elimination of bacteria, which is considered the main cause of endodontic disease (1), and the elimination of periapical disease or its prevention (2).

Therefore, cleaning and debridement of the root canal system by mechanical instrumentation and irrigation is considered the most crucial part in the treatment of an endodontic infection and its prevention. These processes allow the removal of all necrotic tissue, bacteria, and dentin debris. In addition, they give the root canal a shape and taper that allows easy cleaning, placement of medication, and obturation.

In endodontic practice, the instrumentation of a root canal during treatment is usually a demanding element and is quite time consuming.

Over the last 20 years, nickel-titanium (NiTi) rotary files became an integral part in the instrumentation of root canals and one of the most important armamentariums of endodontic therapy, changing how dental practitioners envisioned instrumentation. The widespread use of NiTi files among dentist and specialist is attributed to their favourable qualities and ability to facilitate root canal treatment and to fulfil the biological objectives of root canal treatments.

## 1.2 History of NiTi

Until the early 1990s, root canal treatment was conventionally performed by stainless steel files; these were more resistant to cyclic fatigue and torsional failure when compared to carbon steel instruments (3, 4). Unfortunately, this type of instrument had a tendency to alter the natural curvature of the root canal due to its stiffness, resulting is procedural mishaps such as transportation, zipping, and perforation.

The development of NiTi in 1960, by Sir William F. Buehler – a metallurgist at a naval ordnance laboratory in Maryland, USA, proved to be a huge advancement in the fabrication of endodontic files. Buehler was in search of a metal that was water and salt resistant, and at the same time nonmagnetic, that was suitable for naval use in a space program underway at that lab (5). A number of years later, in 1988, this alloy was introduced into the field of endodontics by Dr Harmeet Walia (6), where he anticipated the use of NiTi orthodontic wires for fabricating endodontic files. Those NiTi files were discovered to have twice, or more, the flexibility of a stainless-steel file and much higher resistance to torsional fatigue.

NiTi alloy has a vast range of beneficial qualities that make it an efficient material for use in rotary file instruments.

## 1.3 Composition, Structure, and Properties of NiTi

Nickel-titanium alloy is considered an unusual alloy, this is because it does not conform to the known rules of metallurgy. It was originally named Nitinol, because of the elements of which the material was composed; Ni for nickel, Ti for titanium, and nol from the Naval Ordnance Laboratory (5).

Endodontic NiTi files are composed of nickel (56 wt%) and titanium (44 wt%), with trace elements of iron, copper , oxygen , chromium , cobalt and carbon totaling less than 1% (6). The combination is a near to one-to-one atomic ratio (equiatomic) of the main elements, nickel and titanium.

NiTi can exist in two temperature-dependent crystalline structures and in a third intermediate phase, which is called the R-phase. At high temperatures (approximately 100 °C), it exist as a stable body-centered lattice called the austenite phase, or parent phase – because it can be recovered when the alloy is heated above a certain temperature (7); the NiTi alloy is hard and strong in this phase (7). At lower temperatures the material is in its martensite form, which is a monoclinic crystalline lattice, also called daughter phase; it is ductile and soft and can easily be deformed.

When the NiTi alloy in the martensite phase is heated, it transforms into the austenite phase. The temperature at which this phenomenon starts is called the austenite start temperature ($A_s$) and it ends at a temperature that is called the austenite finish temperature ($A_f$). At, and above, this temperature range the NiTi alloy has completed its shape memory and will display its superelasticity. However, when the austenite is cooled, it transforms into the martensite alloy; the temperature at which this phenomena begins is called the martensite start temperature ($M_s$) and it ends at the martensite finish temperature ($M_f$) where it returns back to the austenite phase (8).

The R-phase has a rhombohedral crystalline lattice structure. It usually forms under specific conditions, as an intermediate transition between the austenite and martensite phases (7,9,10). This intermediate phase usually occurs during a very narrow range of temperatures of the cooling or heating transitions between austenite and martensite (10).

The crystalline structure of the NiTi alloy can be altered by either stress or temperature variance. This is of the utmost importance, because the properties of the two crystalline structure forms are notably different; thus, this determines their mechanical properties (8,10).

NiTi alloys with nearly equiatomic ratios possess unique super elasticity and shape memory effects, these two properties are almost exclusive to nickel-titanium alloy (7). Shape memory, a distinguishing feature of NiTi related to temperature changes, is defined by the ability of the metal to return to its parent phase once above the transition finish temperature (8). On the other hand, super elasticity is associated with a phase transformation of the alloy when stress is applied above a critical level – it usually happens when the temperature is above the austenite finish ($A_f$) temperature of the material. This stress-induced martensitic transformation usually reverses spontaneously upon release of the stress; at this point the material returns to its original shape and size (8,10).

## 1.4 Differential Scanning Calorimetry (DSC) Analysis

Differential scanning calorimetry (DSC) analysis is a technique that was first introduced to the endodontic field by Brantley et al.; it is a thermoanalytical technique that is used to evaluate phase transformation temperature of rotary NiTi endodontic instruments (11). It measures the change in the heat flow, which is usually associated with the austenitic and martensitic phase transformations through a cooling/heating cycle. The transformations are usually detected as exothermic peaks on the cooling DSC curves and endothermic peaks on the heating DSC curves. This technique gives a prediction of which phase of the NiTi alloy exists at a given temperature. Brantley et al. (11) found the austenite finish temperature ($A_f$) was 25°C for traditional NiTi

files, which indicated that the files would be completely in the austenite phase at room temperature.

## 1.5 Mode of Fracture of NiTi Rotary Files

Despite the major advantages of NiTi rotary files, instrument fracture is a common occurrence and is of major concern in clinical use.

The frequency of file fracture was reported to be 21% according to a study conducted over 6 months, where 378 Quantec files were collected from endodontic practices (12). Conversely, a lower frequency (5%) of file fractures were reported in an examination of used and discarded NiTi files gathered from 14 endodontists in four countries (13). A total of 7,159 NiTi files were examined for defects. Unwinding was found to be in 12% of the files and fractures in 5% (3.5% flexural, 1.5% torsional).

Fracture of endodontic files is usually classified into two types: cyclic fatigue failure and torsional failure, with cyclic fatigue failure being the main reason for file fracture during clinical use (14). Separation of NiTi Usually occurs due to cyclic fatigue failure specifically in curved roots, where half of the file is under tension on the outside of the curvature of the root and the other half is under compression on the inner side of the root; the stress is mainly concentrated in the curvature of the root (15).

There are a several risk factors that leads to cyclic fatigue failure: angle of curvature and an acute radius are two examples of those risk factures (15).

The second situation that may impact file fracture is torsional fatigue. Torsional resistance is evaluated with a torsiometer and usually occurs when the tip of the file gets locked in the canal, while the rest of the instrument continues to rotate – exceeding the elastic limit. Plastic deformation signs can be noticed in this type of fracture.

## 1.6 Cyclic Fatigue Resistance Testing

To date, there is no international standard, nor specifications, to test the cyclic fatigue resistance of endodontic NiTi rotary files. The American National Standards Institute/American Dental Association (ANSI/ADA) specification No. 28 has not identified a standard test for cyclic fatigue (16).

Four methods were described in an article by Cheung to investigate fatigue resistance fractures *in vitro* (17):

1) The curved metal tube method: A study done by serene et al (18) tested NiTi files by rotating them in a curved metal tube without binding until they broke. Subsequently, Pruett et al. (15) standardized the radius of curvature of the testing tube, reaching the conclusion that the radius of curvature affected the fatigue life more than the angle of curvature. Further studies were performed using the same method, while changing the diameter of the tube or using glass tubes instead of metal. This method had a major drawback in that the same tube was used for various sizes; in this case small files would be subjected to less strain than large instruments, resulting in greater fatigue resistance for smaller instruments.
2) The grooved block-and-rod assembly method: This method was first suggested by Haikel's group (19) to test stainless-steel files. It consists of a V-shaped groove, simulating a root

canal, in a steel block with a size-matched steel rod, the confined file rotates freely in the groove. This design had the same issue as that of the curved metal, which is that the degree of fit within the groove can affect the curvature; thus, the strain imposed on the file can't be accurately evaluated.

3) The rotation against an inclined plane method: this type of fatigue testing examined the fatigue resistance of NiTi files by running them against an inclined, polished, metal surface (20). The angle of inclination was changed to control the radius of curvature of the file. This method is easy to set up and can also provide pecking movement simulating vertical movement done in vivo. The drawback is that the surface strain is difficult to estimate because the radius of the file curvature cannot be derived from the angle of inclination. This test did not provide any definite relationship between the fatigue resistance and the angles of the inclined plane of the model.

The 3-point bend of a rotating instrument method: This method is considered a recent technique in endodontic literature. It has been proposed to overcome all the disadvantages of the previously explained methods (21). In this technique the model consists of three smooth cylinder-shaped stainless-steel pins that are attached to acrylic shims with a changeable horizontal direction. In this technique the file curvature will be determined by the position of the pin. The restraint in this technique will produce a circular curvature (22).

In conclusion, each of these cyclic fatigue testing methods had their own limitations. However, in order to fully comprehend the nature of the metal alterations and also specifically their impact on increasing the resistance to fatigue, an international standardization of the cyclic fatigue testing of NiTi rotary files should be developed so the results can be compared (17).

## 1.7 Fractography

Electron scanning microscopy of the NiTi file surface fractured due to cyclic fatigue usually shows a couple of characteristic features. In 1997, a study done by Pruett et al. described the stages that NiTi undergoes during cyclic fatigue fracture (15). Stage one started with crack initiation, usually located at the periphery of the instrument. Pruett described this area as being smooth and featureless. Stage two involves propagation through striations; these striations represent the progression of the crack. The third and final stage is the rapid zone of fracture or ultimate ductile fracture, which is characterized with dimpling and micro-voids.

## 1.8 The Five Generations of Nickel Titanium Rotary Files

The introduction of rotary NiTi files occurred in the 1990s (23). At that time, most of the rotary files had a noncutting, round tip that was meant to act as a guide in the root canal. The file design changed through time and progress has been made in the alloy processing and manufacturing technique.

The first rotary file was designed by Dr. John McSpadden, a well-known inventor and researcher. It was introduced into the market in 1992. This new file was characterized by having a fixed taper with a non-cutting radial land. This design marked the first generation of the rotary systems (23).

Within a few years, by the end of the 1990s, a second-generation rotary file system (23) was introduced, reducing the need for numerous files to clean and shape the root canal system. It was

characterized by having a cutting active edge without a radial land feature and variable tapers. Examples of the second-generation rotary NiTi files include ProTaper Universal, K3, and BioRaCe.

Subsequently, several attempts were made to enhance the fatigue resistance of the rotary NiTi files, which led to third-generation files. These new files were thermomechanically treated, where improvements in metallurgy enhanced their properties. Thermomechanical processing increased the transitional temperature; therefore, increasing the files' flexibility and resistance, enhancing their microstructure.

NiTi files such as Hyflex CM, Vortex Blue, Typhoon, and Twisted files are some of the thermomechanically treated files that have been introduced to the market and are considered examples of third generation NiTi rotary files (23).

Fourth-generation files (23) had the feature of reciprocation motion, which significantly reduced the number of files required to prepare the root canal. These include the Wave One gold system introduced by DENTSPLY Tulsa Dental in 2011 and RECIPROC from the VDW company, both systems are considered a single file shaping technique.

Fifth-generation rotary files were designed with an offset center of rotation. Therefore, during rotation they produce a mechanical wave of motion that goes along the active part of the rotary file. This type of motion minimizes the engagement between the dentin and the file. ProTaper Next and Revo-S are two commercially available examples of this new generation.

## 1.9 Modification of NiTi Files to Enhance Properties

Regardless of the all the advantages attributed to the rotary NiTi files, there is still a need to develop files with enhanced flexibility and cutting efficiency and increased resistance to cyclic fatigue.

Manufacturers have introduced many ways to help improve the properties of NiTi files, such as the integration of heat treatment which offers microstructure control (24). Another attempt is surface engineering such as implantation or electropolishing of NiTi files (24). Implantation was used as an attempt to enhance the surface of the NiTi instrument and to also minimize inherit defects. Many studies suggested using elements such as argon (25), nitrogen (25), and boron (26). Implantation of argon and boron ions gave promising results with some instruments – contrary to use of nitrogen ions, which gave mixed results. Another method is plasma immersion, which resulted in increased wear resistance according to Alves-Carlos et al. (27).

Another method that was attempted is electropolishing, which was studied by many authors, including Cheung (17). It is mainly used for surface finishing of metallic medical appliances. This method often changes the surface composition and texture of the instrument, making it more homogenous and providing it with an oxide layer that acts as a protective layer. This method provided reduced surface defects and residual surface stress.

In the past two decades a couple of studies found that changes in transformation behaviour through heat treatment were a very effective method in increasing the fatigue resistance and flexibility of NiTi rotary files (28).

M-wire which is a modification of the super elasti508 NiTi, introduced by Dentsply Tulsa dental specialties in 2007, was produced by a method where a series of heat treatments were applied to NiTi wire blanks; ProFile GT series X, Vortex Blue, and ProFile Vortex are some of the NiTi files fabricated from M-wires. Johnson et al. reported that the cyclic fatigue resistance of the file made of M-wire with a ProFile design was 400% more resistant than traditional NiTi files of the same size (29).

Controlled memory (CM) wire was introduced in 2010 by DS Dental. This novel alloy was manufactured using a special thermomechanical process that controls the memory of the material rendering it super flexible without the shape memory of the traditional NiTi files, examples of these files include TYPHOON (TYP CM; Clinician's Choice Dental Products, New Milford, CT) and Hyflex CM (HyFlex; Coltene Whaledent, Cuyahoga Falls, OH) . It was found that files fabricated from CM wire were almost 300–800% more resistant to fatigue failure than traditional NiTi files when studied in a 3-point bending technique in dry conditions (30).

## 1.10 New EndoSequence Controlled Memory Files

The EndoSequence CM file was introduced to the market in 2018, see Figure 1. They are manufactured with enhanced metallurgy and a special heat treatment process that permits cutting edge fidelity and better resistance to cyclic fatigue. EndoSequence CM provides endodontist with a file with superior flexibility and significantly more resistance to separation (31).

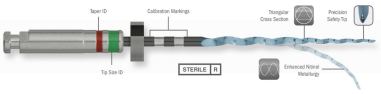


**Figure 1** EndoSequence controlled memory file (Brassler, USA).

# Chapter 2:

## 2.1 Objectives

- To compare the cyclic fatigue resistance of heat-treated files (ESCM, K3XF, VB) to traditional files (ES, K3) in five different curvature location.
- To evaluate the phase transformation behaviour of EndoSequence Controlled Memory (ESCM) files and compare it to the predecessor files (EndoSequence; ES) using DSC analysis.

## 2.2 Null hypotheses

- There is no difference in the cyclic fatigue resistance between the ESCM and ES traditional file in the five different types of curvatures.
- There is no difference in the cyclic fatigue resistance between the K3 and K3XF files in the five types of curvatures.
- There is no difference in the cyclic fatigue resistance between ESCM and other heat-treated files such as VB and K3XF.
- There is no association between the fractured fragment length and the type of curvature.

- There is no difference in the phase transformation behaviour between the ESCM and traditional ES file.

## 2.3 Material and Methods

### 2.3.1 Sample size calculation (statistical power calculation)

The sample size was calculated using the G* power test version 3.1.9.4 software (Brunsbuttel, Germany). The significance value was set at 0.05, and the power at 80. The software calculated eight files per group; however, 10 files per group were included in the study. The total sample size was 250 files (50 of each file type).

### 2.3.2 Cyclic Fatigue Test

Three heat-treated NiTi files (size 25/.04): ESCM, Vortex Blue (VB) (Dentsply Tulsa Dental Specialties, Tulsa, OK) and K3XF (SybronEndo, Orange, CA) and two superelastic NiTi files: EndoSequence (ES) (Brasseler USA) and K3 (SybronEndo) were subjected to fatigue tests. The artificial ceramic canals were milled using an InCoris ZI zirconium oxide disc (Dentsply Sirona, Bensheim, Germany) and the inLab MC X5 digital computer-aided design and computer-aided manufacturing (CAD/CAM) system (Dentsply Sirona), see Figure 2. The size of the artificial canal was 30/.06 with an angle of 60° and a radius of curvature of 3 mm. The total length of the canal was 16 mm and the arc length was 3.14 mm. The distance between the canal orifice and the location of curvature will be abbreviated as distance from the orifice to the curvature (DOC). There were five different canal groups based on the location where curvature began; these involved DOCs of 5, 6, 8, 10 and 11 mm (Fig 3). The model was fixed in a glass container filled with distilled water (300 mL), which was placed on a hot plate in order to maintain body

temperature (37°C ± 2°C), see Figure 4. A rotary handpiece was stabilized on a supporting device that ensured reproducible and precise insertion of the working part of the tested file into the artificial canal. Ten files for each group were tested. The ES and K3 files were rotated at 300 rpm, while the ESCM, K3XF, and VB files were allowed to rotate at 500 rpm until fracture, as recommended by the manufacturer (Figure 4). The time to fracture (seconds) was recorded and multiplied by the number of rotations per minute to obtain the total number of cycles to failure ($N_f$). The experiment was recorded using a digital video camera with a magnification power that allowed accurate detection of file fracture and registration of the fracture time. The broken files were collected for SEM evaluation.

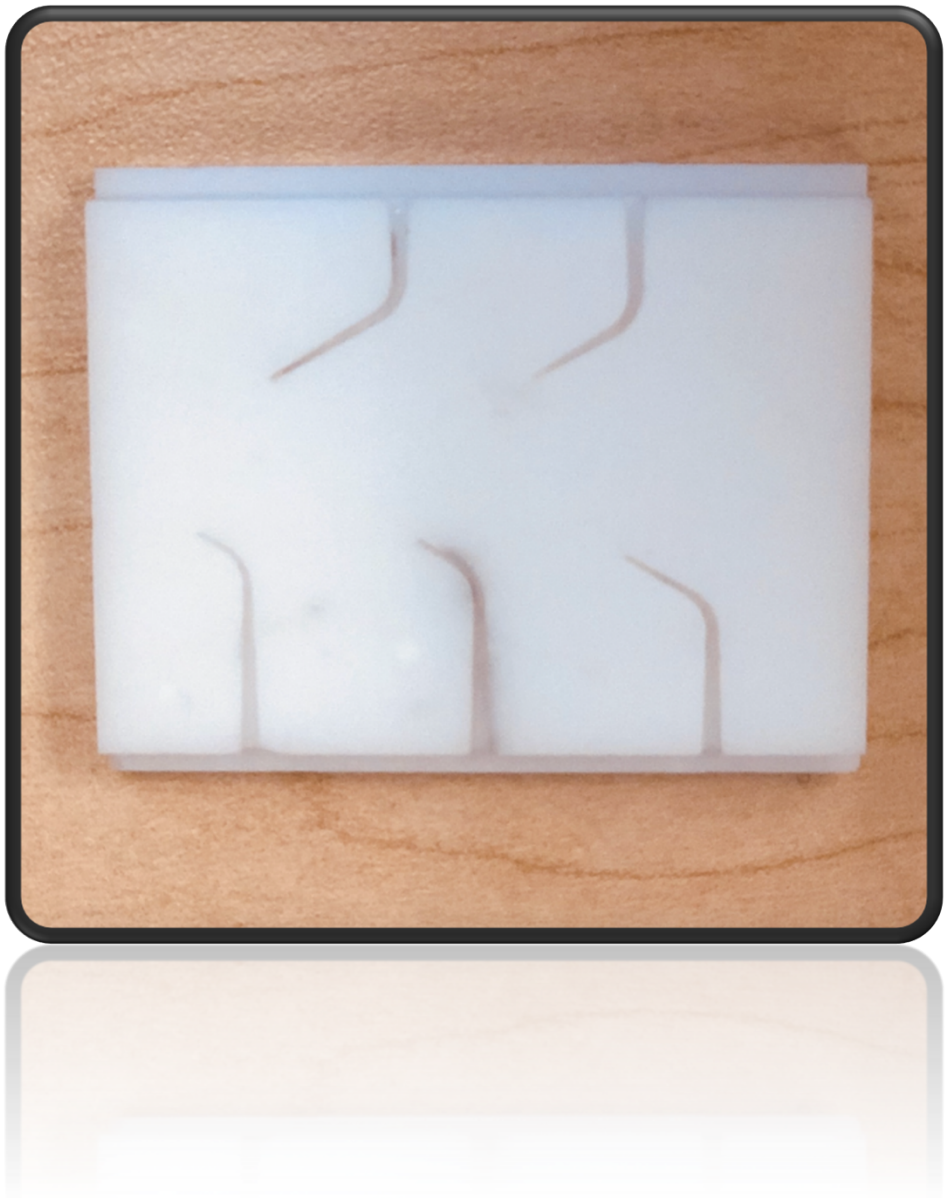

**Figure 2** CAD/CAM study model made of zirconium oxide with five different locations of curvature (5 mm ,6 mm, 8 mm, 10 mm, 11 mm) from the orifice to the location of curvature (DOC).

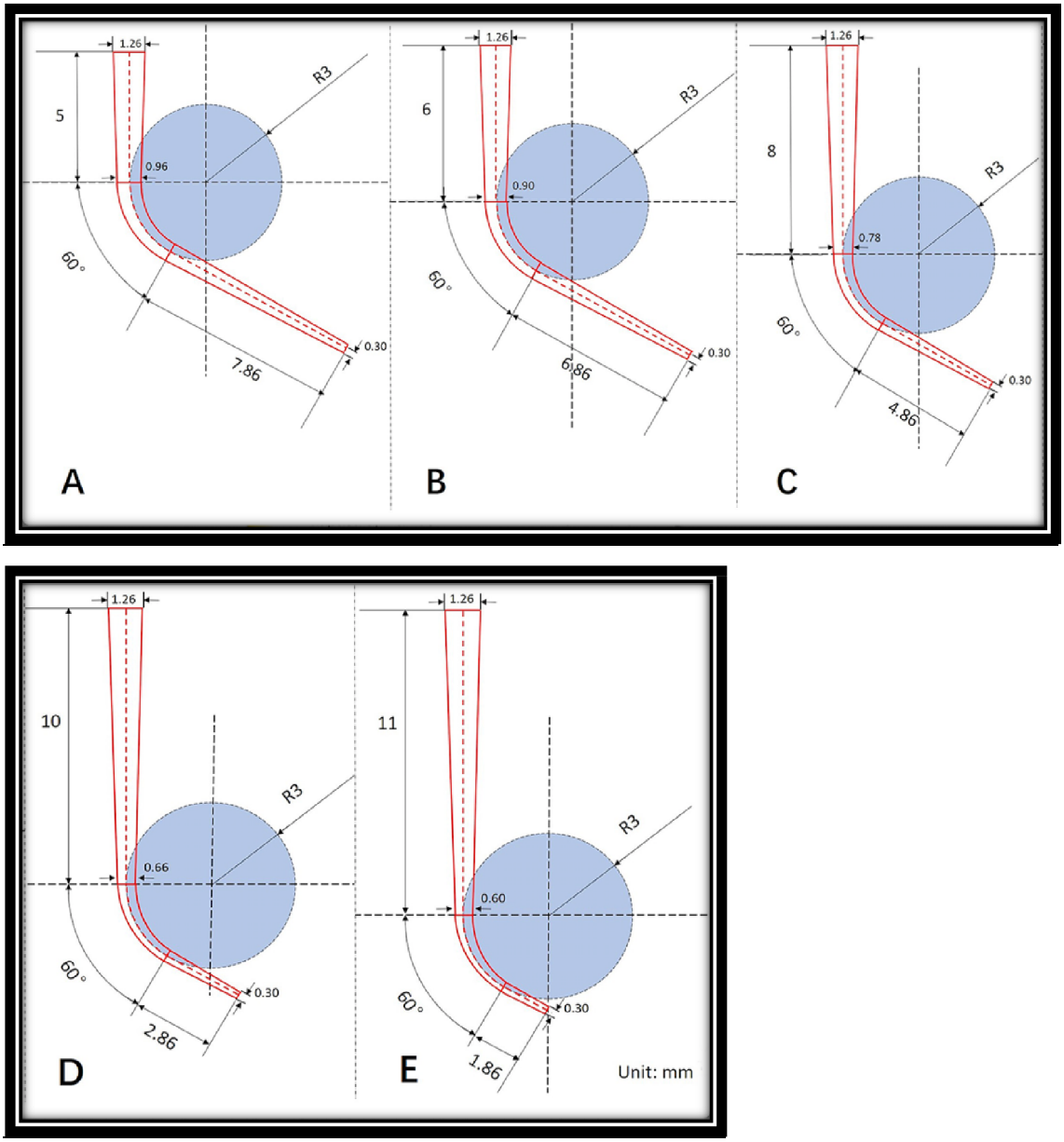


**Figure 3** Schematic drawing of five different locations of curvature: A) 5 mm, B) 6 mm, C) 8 mm D), 10 mm, and E) 11 mm away from orifice of the canal.


**Figure 4** Image of the cyclic fatigue testing device. The test model was fixed in a glass container filled with 300 mL distilled water (37°C ± 2°C).

### 2.3.3 Scanning Electron Microscopy Analysis of the Broken File Surface

The length of the fractured fragments was measured using a stereomicroscope at 10× magnification (Microdissection; Zeiss, Bernried, Germany). Each fractured fragment was collected, and its length measured under magnification by means of a surgical operating microscope (Global, St. Louis, Missouri). Two fragments per group of each file system were randomly chosen for fractographic examination. The fragments were submerged in absolute alcohol (99%) and ultrasonically activated (Endo Ultra, Micromega, Besancon, France) for 60 seconds. The fragments were mounted with the fractured surface facing upwards and submitted for scanning electron microscopy (SEM) analysis (Helios Nano Lab 650; FEI, Eindhoven, Netherlands).

### 2.3.4 Differential Scanning Calorimetry (DSC) Testing

DSC analyses were performed on unused files (Figure 5). To investigate the thermal behavior of the apical and coronal portions of the rotary files, the files were separated into two fragments using a diamond bur under copious amounts of water coolant. The apical fragments, consisting of D0-D5 of the rotary file, and the coronal segments, consisting of D7-D11 of the rotary file, were individually assessed using a Discovery DSC 2500 (TA Instruments, New Castle, USA). Each fragment was weighed with an electronic balance and then placed in a pre-weighed aluminum cell that consisted of a Tzero pan and Tzero Hermetic Lid (TA Instruments, New Castle, USA), see Figure 6. The reference sample was an empty Tzero pan sealed with a Tzero

Hermetic Lid. Using liquid nitrogen, the sample was initially cooled to -80°C. When the sample reached -75°C, it was then heated at 10°C/minute until it reached 100°C. After a brief pause, the sample was then re-cooled to -80°C at a rate of 10°C/min. The data was transferred to TRIOS software (TA Instruments, New Castle), which was used to analyze the thermal behaviour of each specimen. The phase transformation temperatures ($M_s$, $M_f$, $A_s$, and $A_f$) were determined on the thermograms by using the TRIOS software function "Onset Point".

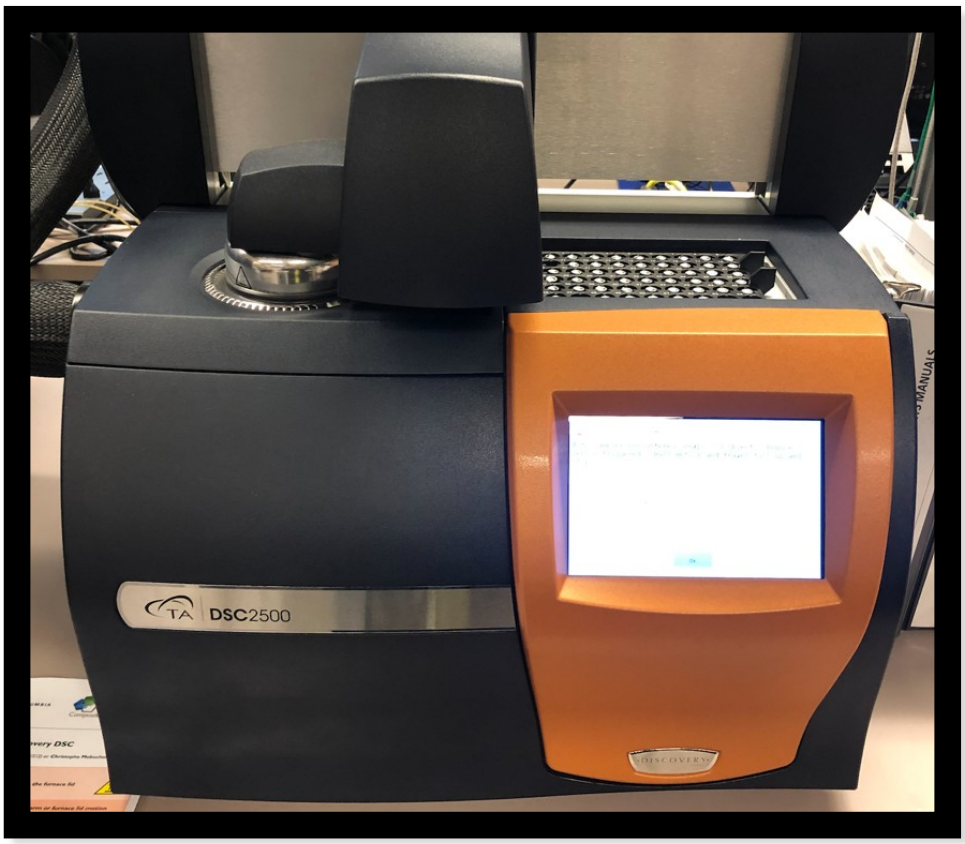


**Figure 5:** Discovery DSC 2500, (TA Instruments, New Castle, USA).

**Figure 6** Image showing aluminum cells of the DSC device, (TA Instruments, New Castle, USA).

### 2.3.5 Statistical Analysis

Statistical analysis was performed using SPSS software (SPSS for Windows version 20.0; SPSS, Chicago, IL). The normality distribution test and the assumption of the homogeneity of variance test were examined using the Kolmogorov-Smirnov test and Levene's test, respectively. One-way analysis of variance (ANOVA) was used to compare the average number of cycles to fracture ($N_f$) of the study groups. Post-hoc multiple comparison with the Tukey test was used to identify and confirm statistically significant differences between groups. The Kruskal-Wallis test was used in this study to compare the mean fragment lengths between groups. Multiple linear

regression analysis was used to examine the potential predictors/explanatory factors associated with the outcome variable ($N_f$). The statistical significance level was set at $p < 0.05$.

## 2.4 Results

### 2.4.1 Cyclic Fatigue Testing Results

A total of 250 NiTi rotary instruments were tested at a 60° angulation and 3 mm radius of curvature in five different locations of curvature (5 mm, 6 mm, 8 mm, 10 mm, 11 mm). The higher the number of cycles to failure ($N_f$) the more the instrument had greater resistance to cyclic fatigue. The results of the cyclic fatigue testing are summarized in Figures 7 and 8. In the case of number of cycles to failure $N_f$, the ESCM files were statistically superior to all other file types in all five curvature types tested. When the location of curvature was concerned, the longer the DOC, the higher the fatigue life of all files. The $N_f$ was highest in all groups where DOC was 10 and 11 mm, and lowest in groups where the DOC was 5 and 6 mm ($p < 0.05$), see Figure 7. There is a significant difference in $N_f$ between the ES and ESCM files in the five types of curvature ($p < 0.05$), see Figure 9. The ESCM had a significantly higher $N_f$ thus higher fatigue resistance than the traditional ES. In Figure 10, the K3XF had a higher $N_f$ than the K3 indicating a higher fatigue resistance. As shown in Figure 11, the $N_f$ was significantly higher for the ESCM files in all groups, compared to the VB and K3XF files ($p < 0.05$). As shown in Figure 12, there was a significant difference between the heat-treated files compared to the traditional NiTi files.

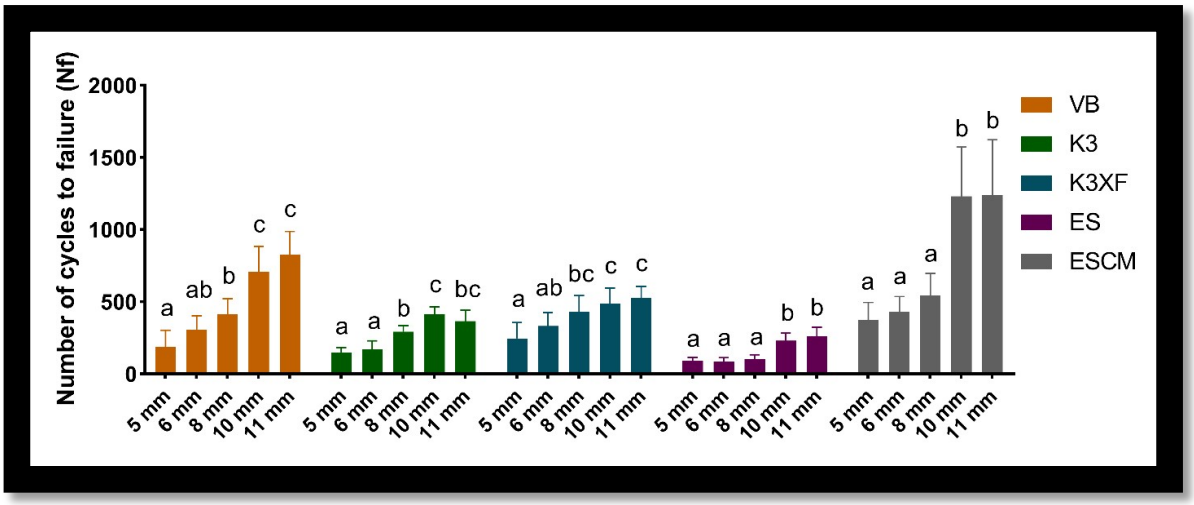


**Figure 7** Graph demonstrating the number of cycles to failure in the five locations of curvature for the five file types (VB, K3, K3XF, ES, ESCM). The ESCM files demonstrated the highest fatigue resistance compared to all other files (K3,K3XF, VB) in five different curvature locations.

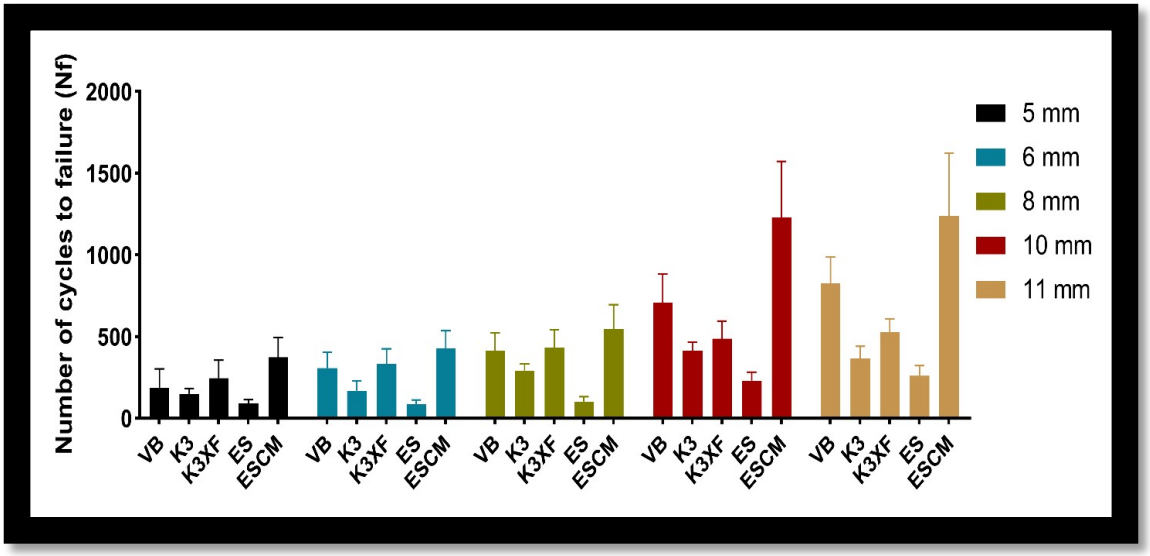


**Figure 8** Graph demonstrating the number of cycles to failure in the five different file types (VB, K3, K3XF, ES, ESCM) in the different curvature locations. The ESCM files demonstrated the highest fatigue resistance compared to all other files (K3, K3XF,VB) in five different curvature locations

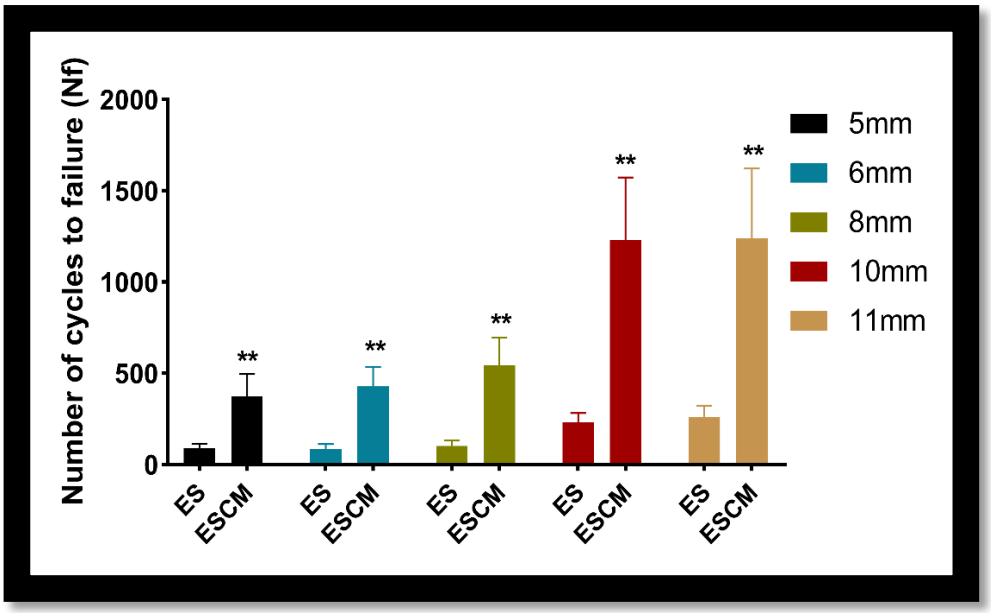


**Figure 9** Graph demonstrating the number of cycles to failure of the ESCM and ES files in the five different locations of curvature; the ESCM file has a significantly higher Nf than ES ($p < 0.05$).

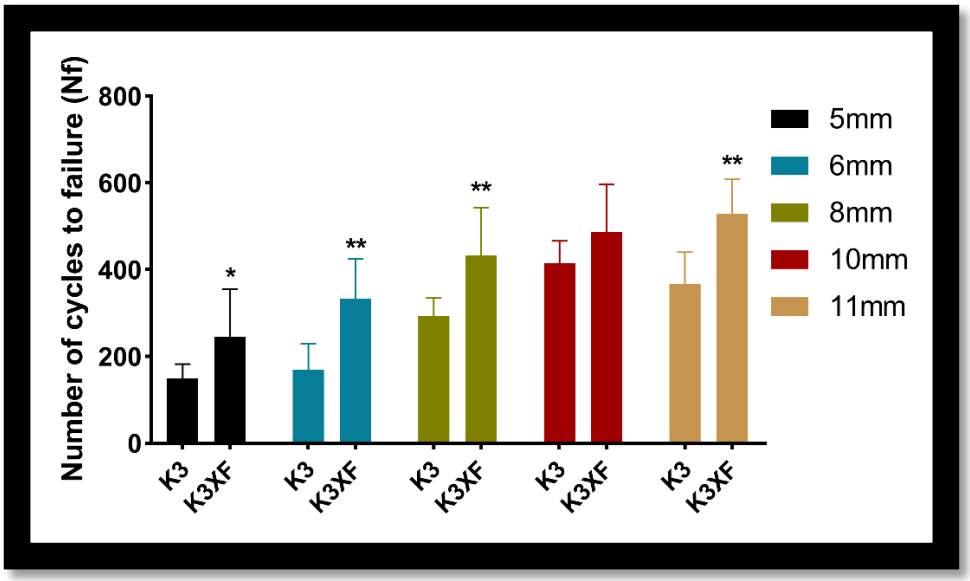


**Figure 10** Graph demonstrating the number of cycles to failure of the K3XF and K3 files in the 5 different locations of curvature; the K3XF file has a significantly higher $N_f$ than K3 ($p < 0.05$).

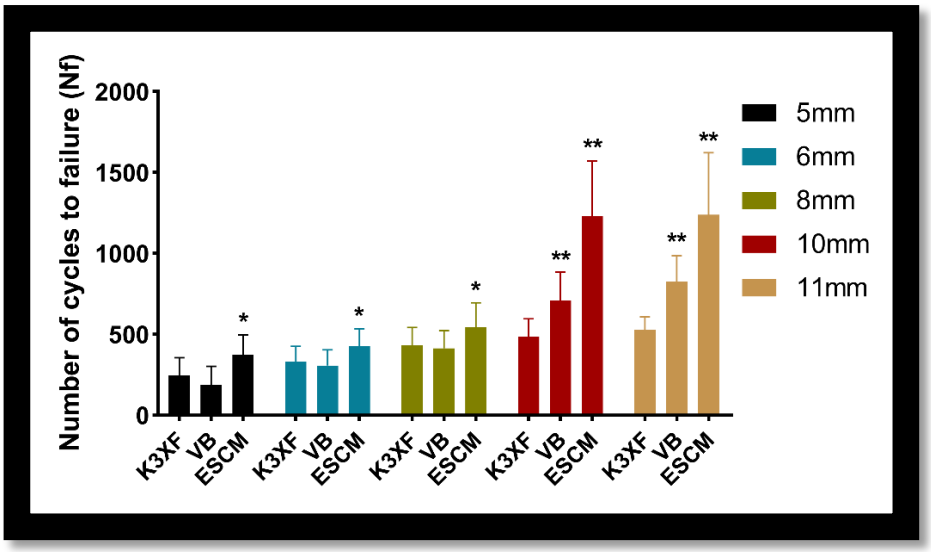


**Figure 11** Graph demonstrating the number of cycles to failure of the heat-treated files (K3XF, ESCM, VB) in the five different locations of curvature; the ESCM has a significantly higher $N_f$ than K3XF and VB ($p < 0.05$).

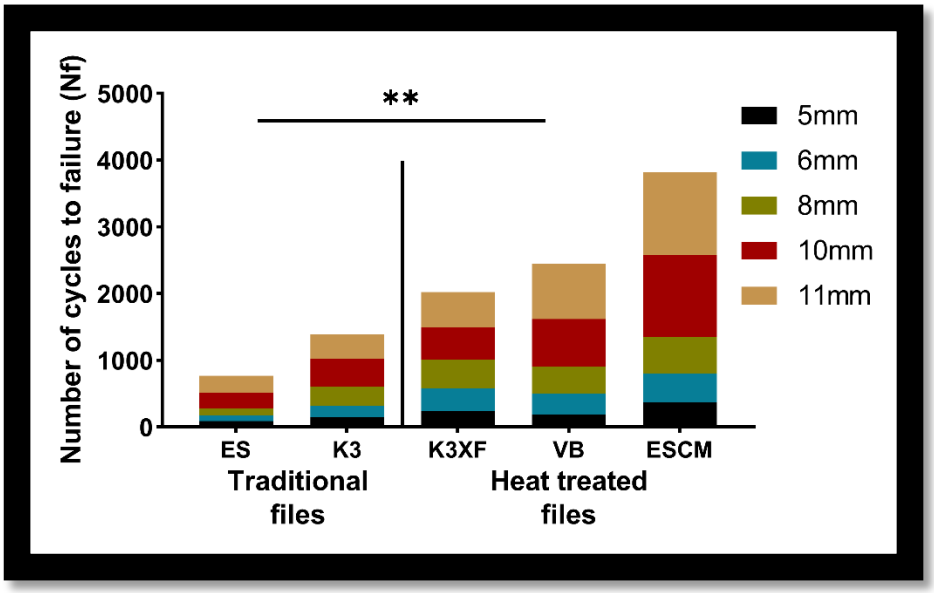


**Figure 12** Graph demonstrating the number of cycles to fracture in the five different files in five different locations of curvature; the results were organized in ascending order to emphasize the difference between heat-treated and non-heat-treated files.

2.4.2 Fractured Fragment Length

The mean length of the fractured fragments for the five types of curvature and the five types of files are displayed in Figure 13. There is no statistically significant difference in the fractured fragment length for the five types of files in each curvature except in the 10 mm group, where a VB file had the longest fractured fragment. We can conclude from the graph the fracture occurred at the point of curvature.

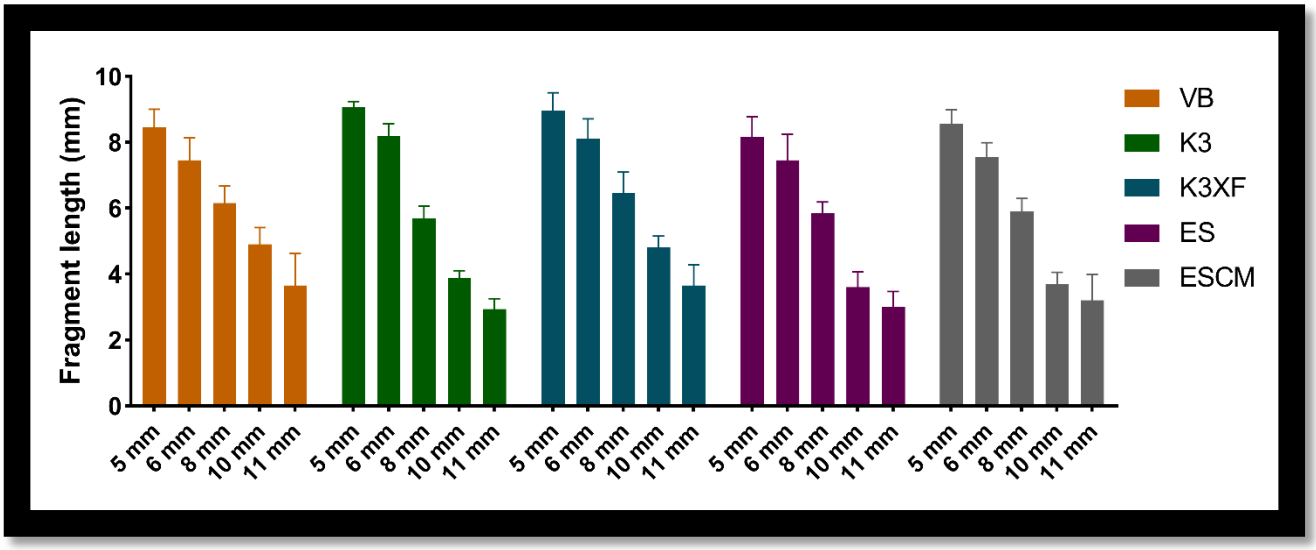


**Figure 13** Graph demonstrating the length of the fractured fragment in the five different locations of the curvature. There is no significant difference in the fractured fragment length in the five types of files in each curvature, except in the 10 mm one.

2.4.3 Predictor Values

Regarding the predictor values, the multiple linear regression test was used to test the association of the $N_f$ with the file type and curvature location. The results showed both the file type and the curvature location significantly ($p < .001$) affected the $N_f$, decreasing the cyclic fatigue resistance of the files.

2.4.4 Fractographic Examination

The surfaces of the fractured files (K3, K3XF, ES, ESCM, VB) all demonstrated evidence of cyclic fatigue failure, starting with crack initiation, then fatigue striation lines, and finally dimpling areas, see Figure 14. Examination were performed using scanning electron microscopy.

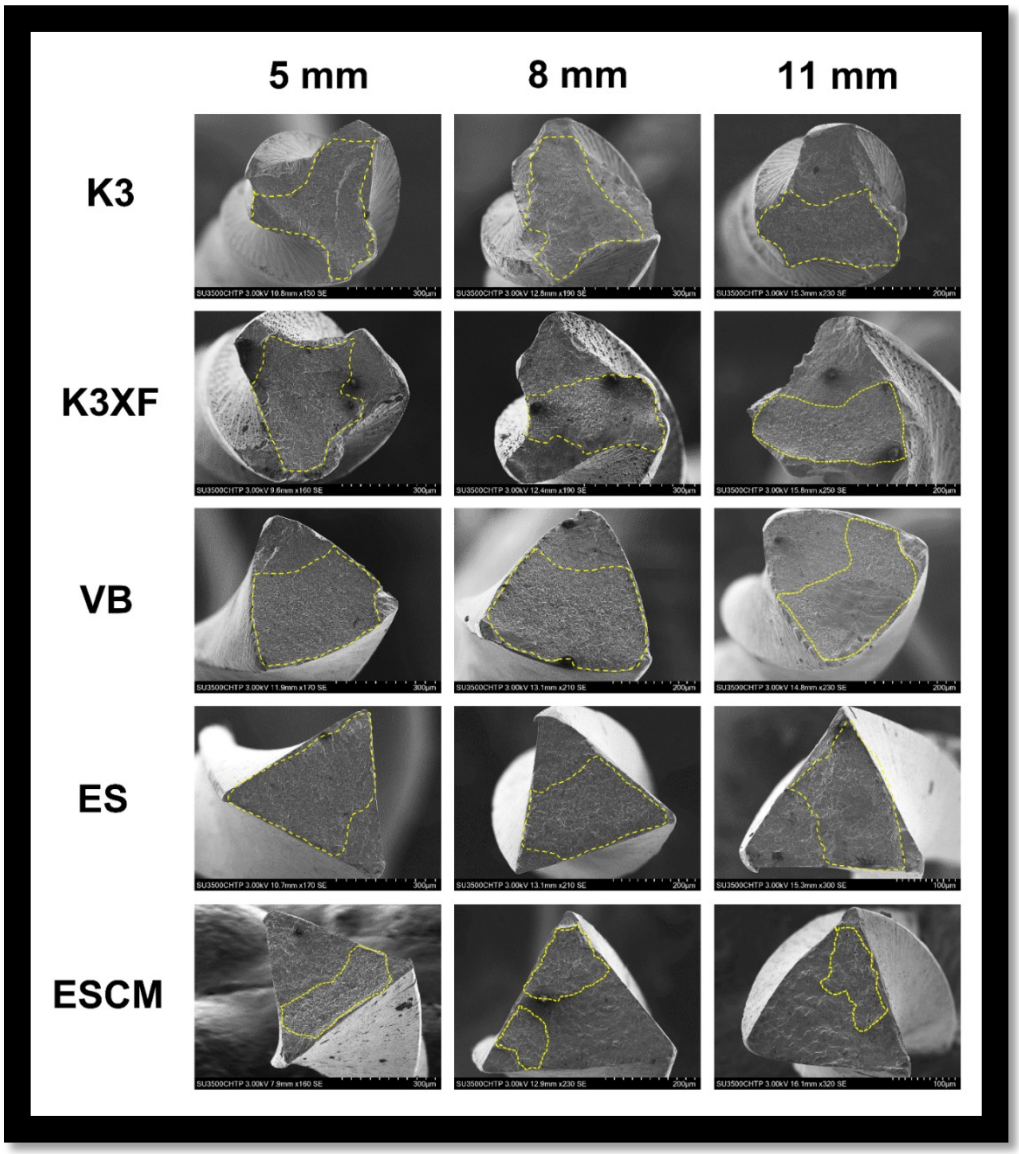


**Figure 14** Photomicrograph of a fractured surface of K3, K3XF, VB, ES, and ESCM files with features of cyclic fatigue failure (crack origin, crack propagation, and dimple area). The fracture starts as one crack or more at the cross-section peripheries, then propagates slowly until complete fracture occurs in the rapid zone of fracture. The dotted area outlines the dimple area, a characteristic feature of cyclic fatigue fracture.

### 2.4.5 Differential Scanning Calorimetry Results

The phase transformation temperatures acquired during the DSC heating and cooling phases of the file fragments (apical, coronal) are presented in Table 1. The mean phase transformation temperatures and standard deviations of the NiTi files when the apical and coronal parts were combined into one group are presented in Table 2.

**Table 1** The phase transformation temperatures acquired during the DSC heating and cooling phases of the file fragments (apical, coronal) of (ES, ESCM, VB, K3, K3XF).

| **System-fragment** | **As (°C)** | **Af (°C)** | **Ms (°C)** | **Mf (°C)** |
|---|---|---|---|---|
| **ESCM 1-apical** | 21.16 | 39.88 | 29.94 | 27.15 |
| **ESCM 1-coronal** | 22.78 | 37.84 | 30.17 | 26.79 |
| **ESCM 2-apical** | 20,81 | 39.21 | 30.65 | 26.14 |
| **ESCM 2-coronal** | 26.38 | 40.89 | 31.07 | 25.85 |
| **ES 1-coronal** | -12.75 | 31.46 | 29.3 | -1.98 |
| **ES 1-apical** | -9.76 | 24.72 | 28.85 | -1.74 |
| **ES 1-coronal** | -10.62 | 32.9 | 26.66 | 1.95 |
| **ES 1-apical** | -13.3 | 32.6 | 32.01 | -2.96 |
| **VB 1-coronal** | 31.37 | 38.09 | 31.41 | 21.94 |
| **VB 1-apical** | 30.41 | 39.29 | 30.58 | 23.8 |
| **VB 1-coronal** | 31.54 | 38.58 | 31.69 | 23.86 |
| **VB 1-apical** | 29.78 | 39 | 30.36 | 24.38 |

| | | | | |
|---|---|---|---|---|
| **K3 1-coronal** | -7.24 | 17.59 | 12.66 | -9.55 |
| **K3 1-apical** | -9.62 | 16.63 | 17.82 | -9 |
| **K3 1-coronal** | -9.62 | 16.63 | 17.82 | -9 |
| **K3 1-apical** | -8.5 | 17.85 | 21.41 | -6.77 |
| **K3XF 1-coronal** | -6.4 | 24.44 | 21.1 | 13.66 |
| **K3XF 1-apical** | -1.49 | 23.5 | 19.7 | 16.23 |
| **K3XF 1-coronal** | -1.51 | 22.79 | 20.74 | 16.57 |
| **K3XF 1-apical** | -3.31 | 23.66 | 25.07 | 18.15 |
| As = Austenite transformation start temperature. Af = Austenite transformation finish temperature. Ms = martensite transformation start temperature. Mf = Martensite transformation finish temperature. | | | | |

**Table 2** Mean phase transformation temperatures and standard deviations of the NiTi files when the coronal and apical fragments were combined into one group.

| **File type** | **As (oC)** | **Af (oC)** | **Ms (oC)** | **Mf (oC)** |
|---|---|---|---|---|
| **ECM** | 23.44 ±2.18 | 39.46±1.3 | 30.46±0.44 | 26.48 ±0.51 |
| **ES** | -11.61 ± 1.46 | 30.42±3.33 | 29.21±1.90 | -1.18±1.87 |
| **VB** | 30.78±0.72 | 38.74±0.45 | 31.01±0.55 | 23.50±0.93 |
| **K3** | -8.75±0.98 | 17.18±0.55 | 17.43±3.12 | -8.58±1.07 |
| **K3XF** | -3.18±2.00 | 23.60±0.59 | 21.65±2.04 | 16.15±1.61 |

Figures 15 and 16 represent the DSC curves for the heating and cooling cycles of the traditional EndoSequence file and the K3 file. In general, the heating curve is usually situated at the upper part of the figure and the cooling curve at the lower part. The typical DSC plot for traditional

superelastic rotary NiTi files (ES, K3) was shown to have a single low defined peak upon cooling and heating, respectively. The austenite finish ($A_f$) temperatures for the traditional superelastic rotary NiTi files (ES, K3) were lower than body temperature (37°C). The mean $A_f$ temperatures for the ES and K3 files were 30.42°C and 17.18°C, respectively. Figure 17 features the VB DSC plot which shows a single defined peak upon cooling and a double endothermic heating curve, the same results were also found in in the DSC curves of the K3XF (Figure18). The mean $A_f$ temperatures for the VB and K3XF files were 38.74°C and 23.60°C, respectively.

In Figure 19, the ESCM NiTi rotary file DSC plot demonstrated a double endothermic peak on the heating curve, which represents the transformation from martensite to the R-phase, followed by transformation from the R-phase to the austenite phase. On the cooling cycle, one well defined peak was detected. The mean $A_f$ temperature was 39.46°C.

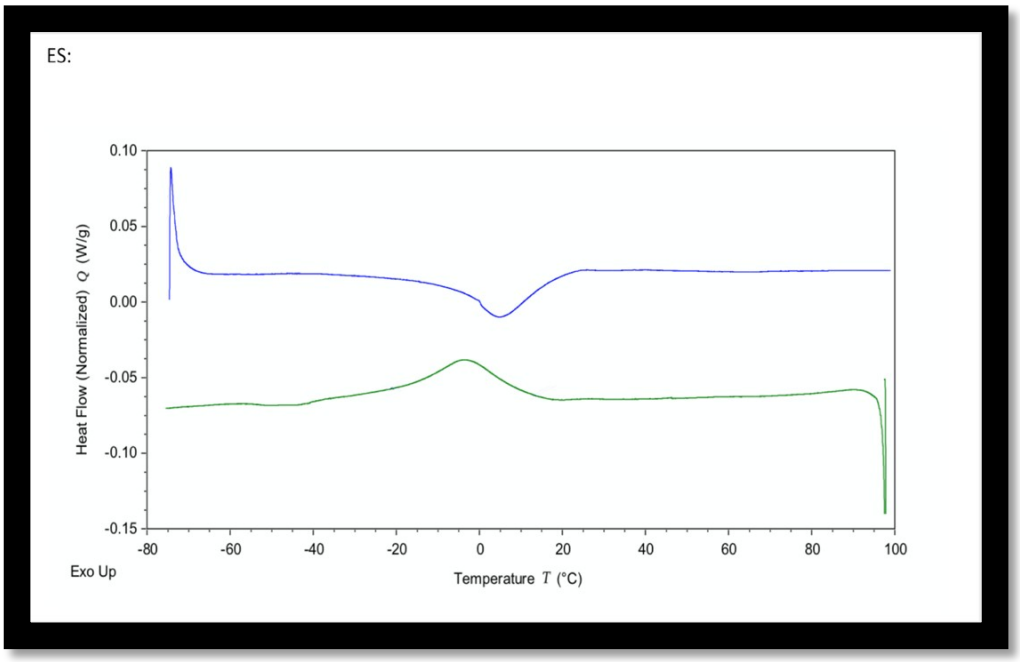


**Figure 15** DSC plots showing heating and cooling curves of a traditional EndoSequence file

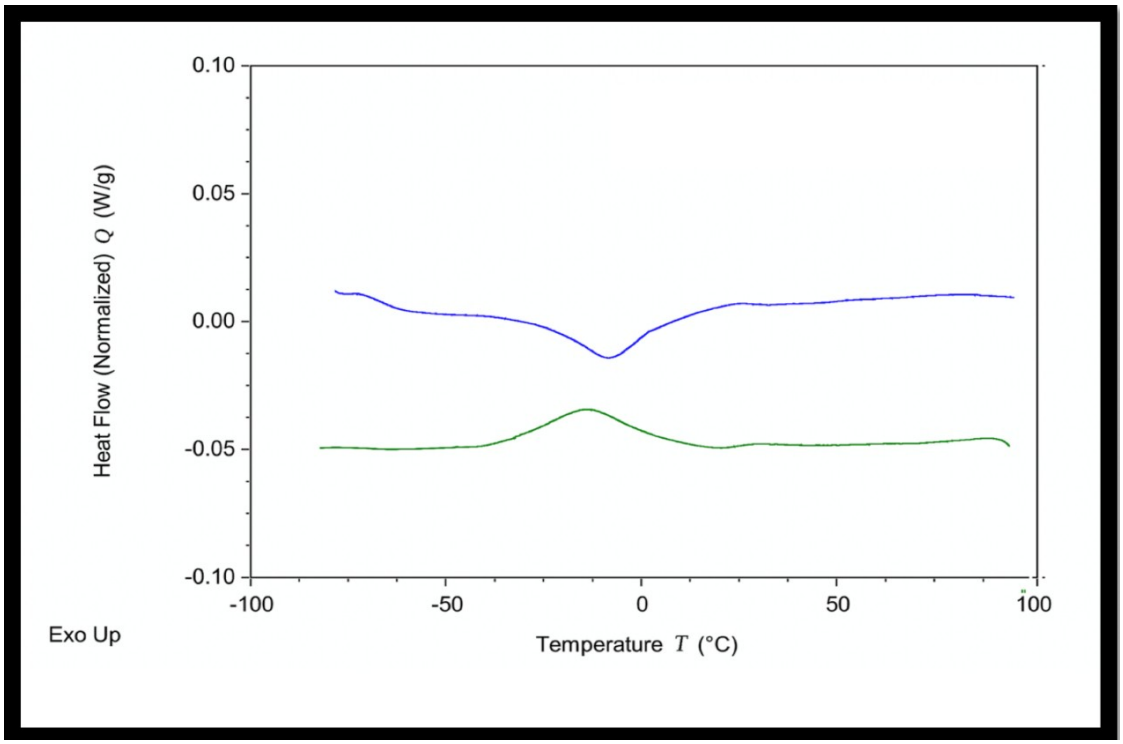


**Figure 16** DSC plots showing heating and cooling curves of a traditional K3 file.

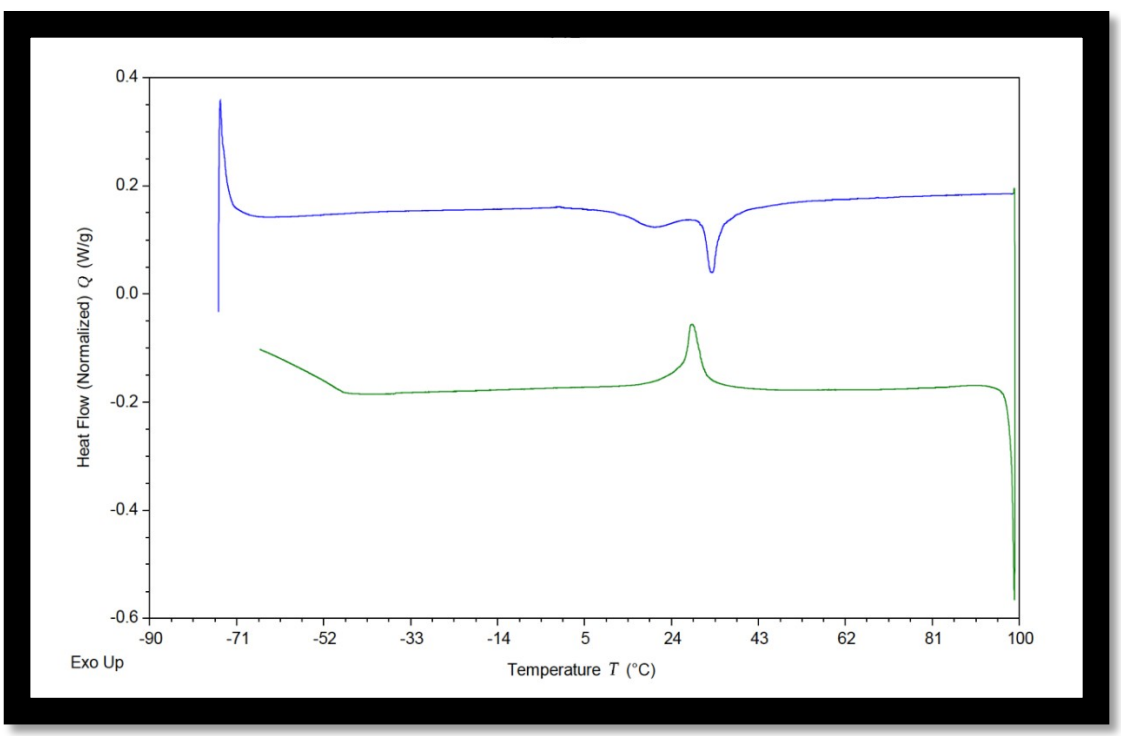


**Figure 17** DSC plots showing heating and cooling curves of a VB file

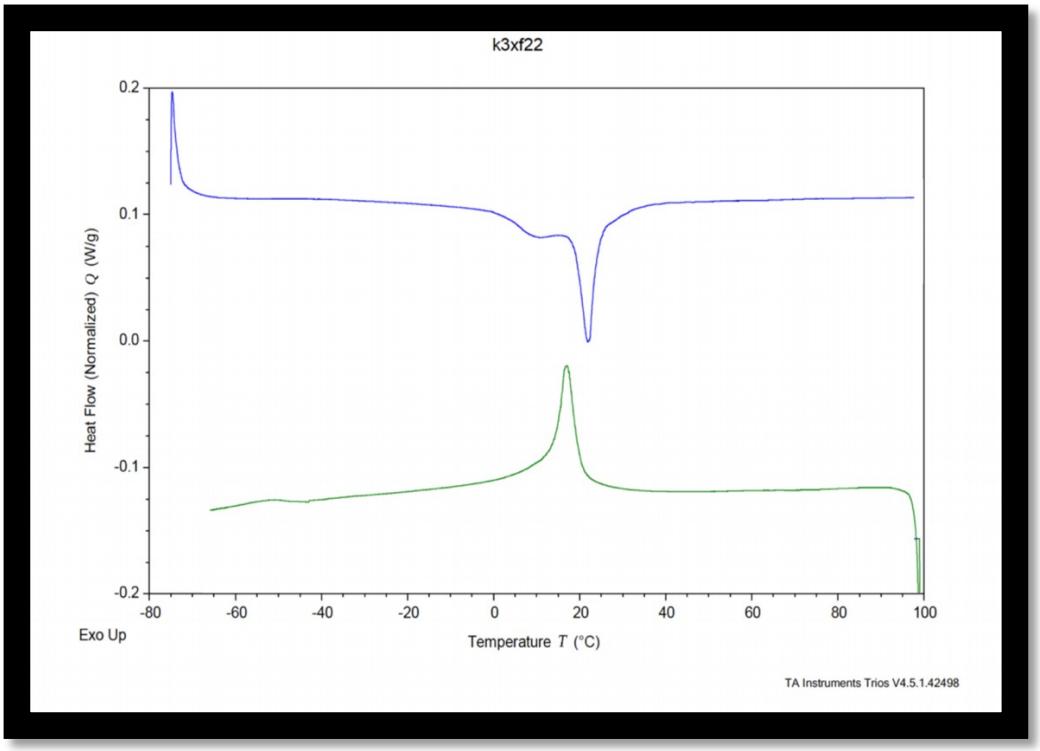


**Figure 18** DSC plots showing heating and cooling curves of a K3XF file.

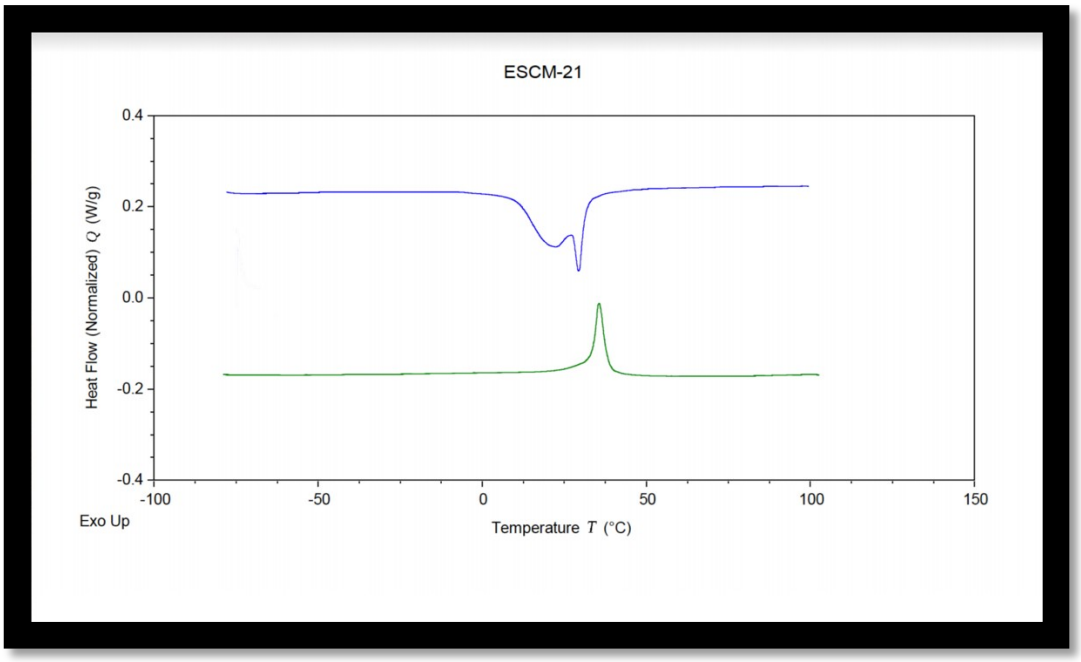


**Figure 19** DSC plots showing heating and cooling curves of the ESCM file.

## 2.5 Discussion

It is well known that both the angle of curvature and the radius are the main determinants of fatigue resistance of NiTi rotary files (15, 32) . In this study, the effect of curvature location on the fatigue resistance of three heat-treated and two superelastic NiTi files was systematically evaluated in distilled water at body temperature. Our work focused on the study of the fatigue life of NiTi files in different curvature locations that may be encountered clinically; it is the first study that tested the cyclic fatigue resistance in a model with five different locations of curvature in an attempt to simulate all types of root curvature. The five different curvature locations were selected to represent the coronal, middle, and apical curve in a clinical situation. The customized artificial canal sizes were constructed corresponding to the dimensions of the instruments tested (tip size and taper) to ensure a close fit without binding; thus, providing the instrument with a suitable trajectory. In the endodontic literature, only two studies investigated the fatigue resistance of superplastic NiTi files in models with an apical curvature and mid-root curvature in dry conditions(33, 34). In these two early studies, the shape of the artificial canal was a cylindrical curved canal without a taper and the size was 1.5 mm wider than the file. Hence, the files were loose inside the model influencing the trajectory of the file inside the canal.

For a better understanding of the fatigue fracture mechanism, several factors (e.g. the angle and radius of curvature, length of the curve, location of curvature, size of the file, etc.) must be considered; however, the simulation of all these factors in laboratory conditions is difficult. In our model design, the artificial canals were constructed with an angle of 60° and a radius of curvature of 3 mm. The file size (25/.04) was chosen because it is a commonly used size during instrumentation. It is well recognized that the complex anatomical conditions encountered in

clinical situations are not fully reproduced, so this study may help clinicians choose the most appropriate file system for a particular type of canal curvature.

Our study showed that all files had significantly reduced fatigue resistance if the point of maximum curvature was shifted from an apical position to a more coronally-located position. The results appeared to agree with earlier finite element modeling findings which showed the magnitude of stress and strain imposed on the file is influenced by the location of the curvature portion (35) . From a mechanical perspective, files of larger diameter have a lower cyclic fatigue resistance than smaller files of the same design (36). Although the heat-treated NiTi files had higher fatigue resistance than the superelastic NiTi files, as mentioned in previous studies (34, 37), the heat-treated files tested in the artificial canals with coronally located curvature showed a lower number of cycles to fracture, hence lower flexibility and increased risk of fracture. Coronally positioned curvatures encountered clinically render treatment challenging to the clinician and can ultimately lead to unwanted events such as instrument separation. To overcome this difficulty the access cavity can be enlarged to ensure a straight-line access to the canal curvatures (32).

Recently, several studies indicated that the fatigue life of NiTi files showed sensitivity to the testing environments, e.g. temperature, liquid used, etc. (30, 38) . In this study, the fatigue resistance was tested in water, which may not represent an actual clinical situation where sodium hypochlorite is typically used as an irrigant. However, couple of studies (39, 40) indicated that sodium hypochlorite did not significantly affect the fatigue behavior of NiTi files. A series of studies performed in the past couple of decades (28, 41, 42), discovered that the changes that happen in the transformation behaviour of the NiTi alloy due to heat treatment rendered this

alloy more flexible and more resistant to fatigue failure. Heat treatment increases the $A_s$ and $A_f$ temperatures, which indicate the temperatures where the transformation of the metallic structure from martensite to austenite are initiated and completed (37, 40). Enhancement in this field led to the introduction of controlled memory (CM) files from DS Dental in 2010. The CM alloy is a novel alloy with enhanced flexibility that was discovered to be 300-800% more flexible than the traditional NiTi alloy (30). In this study the fatigue resistance of a new EndoSequence CM file was tested for the first time; moreover, the results of this study were consistent with previously mentioned studies(30, 37) that examined the fatigue properties of the CM alloy. The new ESCM file showed a higher fatigue resistance compared to all other heated and non-heated files. The ESCM file in this study exhibited superior performance for the five different locations of curvature compared to the traditional NiTi files examined in this study (ES, K3) and the other heat-treated file such as VB and K3XF. The file type (heat treated or traditional superelastic) was a significant factor when evaluating the number of cycles to failure – this result was in accordance with previous studies(37, 42). The DSC assessment of martensitic conversion temperatures helped to predict the behaviour of NiTi files in different environments(39, 44) . Theoretically, using heat treatment to increase the $A_f$ temperature above 35°C, which is the clinical intracanal temperature (45), can help increase the fatigue resistance of the file. In the current study, the mean $A_f$ for two of the heat-treated files was above body temperature (~ 37°C ± 2°C). The mean $A_f$ values for ESCM and VB were 39.46°C and 38.74°C, respectively. The K3XF files were the exception, with a value of 23.60 C. The ESCM and VB $A_f$ values were higher than the $A_f$ of the traditional superelastic NiTi files (30.42°C for ES and 17.18°C for K3) and may be an explanation as to why the heat-treated NiTi files had higher fatigue resistance than traditional NiTi files in five different curvature locations at body temperature. The DSC

plots demonstrated two overlapping endothermic peaks on the heating plots of the ESCM, K3XF, and VB files, indicating that reverse transformation of the alloy passes through the intermediate R-phase; this reflected the complex phase transformation behaviour tracking back to the manufacturing process. The ESCM files had excellent fatigue behaviour when compared to the other heat-treated files (K3XF and VB). Both the $A_f$ temperature and the amount of martensite participating in the phase transformation may be attributed to the fatigue behaviour of the NiTi files. While detailed information about the thermomechanical treatment history of the ESCM file is not available, it seems that this method of processing is a promising way to gain substantial improvements that enhance the safety of endodontic files. However, other properties of the ESCM files (e.g. cutting efficiency and torsional resistance) need to be evaluated to obtain further understanding of the performance of ESCM files.

## 2.6 Conclusion

ESCM files demonstrated the highest fatigue resistanceat five different curvature locations. All tested files had a low fatigue resistance in canals with middle or coronally located curvatures in comparison with canals with apical curvatures. The ESCM files had a higher fatigue resistance than the traditional ES file as well as the K3XF files compared to the traditional K3 files in five types of canal curvature. The ESCM files had the highest fatigue resistance when compared to the other heat -treated files (VB, K3XF).

The ESCM, K3XF, and VB have higher fatigue resistance than the traditional files (ES, K3). The heat-treated files (ESCM, K3XF, VB) exhibited complex phase transformation behaviour compared to the traditional files (ES, K3).

## References


1. Kakehashi S, Stanley HR, Fitzgerald RJ. The effects of surgical exposures of dental pulps in germ-free and conventional laboratory rats. Oral Surg Oral Med Oral Pathol. 1965 Sep;20:340–349 .

2. Pantera EA. Essential endodontology: prevention and treatment of apical periodontitis. J Dent Educ 2008;72(10):1212–1213.

3. Craig RG, Peyton FA. Physical properties of stainless steel endodontic files and reamers. Oral Surg Oral Med Oral Pathol. 1963;16(2):206–217.

4. Craig RG, McIlwain ED, Peyton FA. Bending and torsion properties of endodontic instruments. Oral Surgery, Oral Med Oral Pathol. 1968;25(2):239–254.

5. Buehler WJ, Gilfrich J V., Wiley RC. Effect of low-temperature phase changes on the mechanical properties of alloys near composition TiNi. J Appl Phys. 1963;34(5):1475–1477.

6. Walia H, Brantley WA, Gerstein H. An initial investigation of the bending and torsional properties of nitinol root canal files. J Endod. 1988 Jul;14(7):346-351.

7. Thompson SA. An overview of nickel-titanium alloys used in dentistry. Vol. 33, Int Endod J 2000 Jul;33(4):297–310.

8. Otsuka K, Ren X. Physical metallurgy of Ti-Ni-based shape memory alloys. Prog Mater Sci. 2005;50(5):511–678.

9. Shen Y, Zhou H-M, Zheng Y-F, Peng B, Haapasalo M. Current challenges and concepts of the thermomechanical treatment of nickel-titanium instruments. J Endod [Internet]. 2013;39:163–72. Available from: http://dx.doi.org/10.1016/j.joen.2012.11.005

10. T. Saburi. Ti-Ni shape memory alloys. In: Otsuka, K. WCM, editor. Shape Memory Materials. Cambridge University Press; 1998. p. 49–96.

11. Brantley WA, Svec TA, Iijima M, Powers JM, Grentzer TH. Differential scanning calorimetric studies of nickel titanium rotary endodontic instruments. J Endod [Internet]. 2002 Aug [cited 2019 Oct 1];28(8):567–72. Available from: http://www.ncbi.nlm.nih.gov/pubmed/12184415

12. Sattapan B, Nervo GJ, Palamara JE, Messer HH. Defects in rotary nickel-titanium files after clinical use. J Endod [Internet]. 2000 Mar [cited 2019 Sep 20];26(3):161–5. Available from: http://www.ncbi.nlm.nih.gov/pubmed/11199711

13. Parashos P, Gordon I, Messer HH. Factors influencing defects of rotary nickel-titanium endodontic instruments after clinical use. J Endod [Internet]. 2004 Oct [cited 2019 Sep 21];30(10):722–5. Available from: http://www.ncbi.nlm.nih.gov/pubmed/15448468

14. Cheung GSP, Peng B, Bian Z, Shen Y, Darvell BW. Defects in ProTaper S1 instruments after clinical use: fractographic examination. Int Endod J [Internet]. 2005 Nov [cited 2019 Sep 21];38(11):802–9. Available from: http://www.ncbi.nlm.nih.gov/pubmed/16218972

15. Pruett JP, Clement DJ, Carnes DL. Cyclic fatigue testing of nickel-titanium endodontic instruments. J Endod. 1997;23(2):77–85.

16. Revised ANSI/ADA specifications No. 28 for root canal files and reamers, type K, and No. 58 for root canal files, type H (Hedstrom). Council on Dental Materials, Instruments, and Equipment. J Am Dent Assoc [Internet]. 1989 Feb [cited 2019 Sep 21];118(2):239–40. Available from: http://www.ncbi.nlm.nih.gov/pubmed/2918154

17. Cheung GSP. Instrument fracture: mechanisms, removal of fragments, and clinical outcomes. Endod Top. 2007 Mar;16(1):1–26.

18. Serene TP, Serene TP, Adams JD, Saxena A (Ashok). Nickel-titanium instruments : applications in endodontics. Ishiyaku EuroAmerica; 1995. p. 112.

19. Haikel Y, Gasser P, Allemann C. Dynamic fracture of hybrid endodontic hand instruments compared with traditional files. J Endod [Internet]. 1991 May [cited 2019 Sep 22];17(5):217–20. Available from: http://www.ncbi.nlm.nih.gov/pubmed/1940741

20. Li UM, Lee BS, Shih CT, Lan WH, Lin CP. Cyclic fatigue of endodontic nickel titanium rotary instruments: static and dynamic tests. J Endod [Internet]. 2002 Jun [cited 2019 Sep 22];28(6):448–51. Available from: http://www.ncbi.nlm.nih.gov/pubmed/12067126

21. Cheung GSP, Darvell BW. Low-cycle fatigue of NiTi rotary instruments of various cross-sectional shapes. Int Endod J [Internet]. 2007 Aug [cited 2019 Sep 20];40(8):626–32. Available from: http://www.ncbi.nlm.nih.gov/pubmed/17459117

22. Wick A, Vöhringer O, Pelton AR. The Bending Behavior of NiTi. J Phys IV. 1995 Dec;5(8,pt2):789–794.

23. Haapasalo M, Shen Y. Evolution of nickel-titanium instruments: from past to future.

Endod Top [Internet]. 2013 Sep [cited 2020 Jan 26];29(1):3–17. Available from: http://doi.wiley.com/10.1111/etp.12049

24. Gutmann JL, Gao Y. Alteration in the inherent metallic and surface properties of nickel-titanium root canal instruments to enhance performance, durability and safety: A focused review. Int Endod J. 2012;45:113–128.

25. Lee DH, Park B, Saxena A, Serene TP. Enhanced surface hardness by boron implantation in Nitinol alloy. J Endod [Internet]. 1996 Oct [cited 2019 Oct 1];22(10):543–6. Available from: http://www.ncbi.nlm.nih.gov/pubmed/9198443

26. Wolle CFB, Vasconcellos MAZ, Hinrichs R, Becker AN, Barletta FB. The effect of argon and nitrogen ion implantation on nickel-titanium rotary instruments. J Endod. 2009 Nov;35(11):1558–1562.

27. Alves-Claro APR, Claro FAE, Uzumaki ET. Wear resistance of nickel-titanium endodontic files after surface treatment. J Mater Sci Mater Med [Internet]. 2008 Oct [cited 2019 Oct 1];19(10):3273–7. Available from: http://www.ncbi.nlm.nih.gov/pubmed/18470705

28. Yahata Y, Yoneyama T, Hayashi Y, Ebihara A, Doi H, Hanawa T, et al. Effect of heat treatment on transformation temperatures and bending properties of nickel-titanium endodontic instruments. Int Endod J. 2009 Jul;42(7):621–626.

29. Johnson E, Lloyd A, Kuttler S, Namerow K. Comparison between a novel nickel-titanium alloy and 508 Nitinol on the cyclic fatigue life of ProFile 25/.04 rotary instruments. J Endod. 2008 Nov;34(11):1406–1409.

30. Shen Y, Qian W, Abtin H, Gao Y, Haapasalo M. Fatigue testing of controlled memory wire nickel-titanium rotary instruments. J Endod. 2011 Jul;37(7):997–1001.

31. brasseler dental group,The perfect Balance of strength and flexibility Endosequence Contorlled memoryfile .US: Brasseler ;2018.

32. Peters OA, Kappeler S, Bucher W, Barbakow F. Engine-driven preparation of curved root canals: Measuring cyclic fatigue and other physical parameters. Aust Endod J. 2002 Apr;28(1):11–17.

33. Lopes HP, Chiesa WMM, Correia NR, De Souza Navegante NC, Elias CN, Moreira EJL, et al. Influence of curvature location along an artificial canal on cyclic fatigue of a rotary nickel-titanium endodontic instrument. Oral Surg Oral Med Oral Pathol Oral Radiol Endod. 2011;111(6):792–796.

34. Lopes HP, Vieira MVB, Elias CN, Gonçalves LS, Siqueira JF, Moreira EJL, et al. Influence of the geometry of curved artificial canals on the fracture of rotary nickel-titanium instruments subjected to cyclic fatigue tests. J Endod. 2013 May;39(5):704–707.

35. Gao Y, Cheung GSP, Shen Y, Zhou X. Mechanical behavior of ProTaper Universal F2 finishing file under various curvature conditions: A finite element analysis study. J Endod. 2011 Oct;37(10):1446–1450.

36. Schneider SW. A comparison of canal preparations in straight and curved root canals. Oral Surg Oral Med Oral Pathol. 1971;32(2):271–275.

37. Zhou HM, Shen Y, Zheng W, Li L, Zheng YF, Haapasalo M. Mechanical properties of

controlled memory and superelastic nickel-titanium wires used in the manufacture of rotary endodontic instruments. J Endod. 2012 Nov;38(11):1535–1540.

38. De Vasconcelos RA, Murphy S, Carvalho CAT, Govindjee RG, Govindjee S, Peters OA. Evidence for reduced fatigue resistance of contemporary rotary instruments exposed to body temperature. J Endod. 2016 May 1;42(5):782–787.

39. Huang X, Shen Y, Wei X, Haapasalo M. Fatigue resistance of nickel-titanium instruments exposed to high-concentration hypochlorite. J Endod [Internet]. 2017 Nov [cited 2020 Jan 14];43(11):1847–1851. Available from: http://www.ncbi.nlm.nih.gov/pubmed/28951027

40. Pedullà E, Grande NM, Plotino G, Palermo F, Gambarini G, Rapisarda E. Cyclic fatigue resistance of two reciprocating nickel-titanium instruments after immersion in sodium hypochlorite. Int Endod J. 2013 Feb;46(2):155–159.

41. Kuhn G, Tavernier B, Jordan L. Influence of structure on nickel-titanium endodontic instruments failure. J Endod [Internet]. 2001 Aug [cited 2019 Oct 8];27(8):516–520. Available from: http://www.ncbi.nlm.nih.gov/pubmed/11501589

42. Hayashi Y, Yoneyama T, Yahata Y, Miyai K, Doi H, Hanawa T, et al. Phase transformation behaviour and bending properties of hybrid nickel-titanium rotary endodontic instruments. Int Endod J [Internet]. 2007 Apr [cited 2019 Oct 8];40(4):247–253. Available from: http://www.ncbi.nlm.nih.gov/pubmed/17284269

43. Al-Sudani D, Grande NM, Plotino G, Pompa G, Di Carlo S, Testarelli L, et al. Cyclic fatigue of nickel-titanium rotary instruments in a double (S-shaped) simulated curvature. J Endod [Internet]. 2012 Jul [cited 2019 Oct 10];38(7):987–989. Available from:

http://www.ncbi.nlm.nih.gov/pubmed/22703666

44. Shen Y, Huang X, Wang Z, Wei X, Haapasalo M. Low Environmental Temperature Influences the Fatigue Resistance of Nickel-titanium Files. J Endod. 2018 Apr 1;44(4):626–629.

454. De Hemptinne F, Slaus G, Vandendael M, Jacquet W, De Moor RJ, Bottenberg P. In vivo intracanal temperature evolution during endodontic treatment after the injection of room temperature or preheated sodium hypochlorite. J Endod. 2015 Jul 1;41(7):1112–5.